Simulation Models Crowd Management

Industrial and Management Engineering, Indian Institute of Technology – Kanpur

Colton Cunov

Undergraduate Researcher

Industrial and Systems Engineering, Texas A&M University

coltoncunov@gmail.com

July 12, 2017

0.0 PREFACE

Two existing models are of interest: the Social Force Model and the Universal Power Law. Experiments and simulations were done to assess the accuracy and similarities of the two models.

1.0 ABSTRACT

One of the widely used model for pedestrian behavior is Social Force Model. Recently, Universal Power Law has also been introduced to model pedestrian behavior in crowded situation [7]. However, some important parameters used in these models lack empirical validation. To optimize these parameters and assess the models' robustness to cultural factors, we collected data from control experiments in Indian context in the simple 2-person, head-on scenario. The models were calibrated using a simulation-based approach and then compared to our observed data.

2.0 PROJECT AIM and STRUCTURE

The aim of the project is to evaluate the effectiveness of the Social Force [10] and Universal Power Law [7] crowd models in the Indian context. We used a small-scale, *head-on* situation to test the models. The major task involved in the current project are as follows:

1. Collect and process 43 sets of video data from the head-on, 2-person situation
2. Evaluate the models' performances as they stand
3. Identify areas of improvement
4. Suggest an alternative model and demonstrate its proficiency

3.0 INTRODUCTION

The Social Force Model, created in its original form over 20 years ago by Dirk Helbing [1], has seen many improvements and adaptations since its inception. It is one of the most ubiquitous crowd models, often serving as a comparison for others. More recently, the Universal Power Law (Karamouzas et. al.) model was introduced as an alternative to the previous approaches based on Social Force Model. These physics-inspired models use a gas-kinetic or fluid-dynamics approach to model the collective behavior of individuals, an idea originally proposed by Henderson [2]. Other approaches of models exist, such as those based on decision rules [4] and artificial intelligence [5],.

3.0 SUMMARY OF SOCIAL FORCE and UNIVERSAL POWER LAW MODELS

3.1 The Model Forces These can be understood by first imagining the i^{th} person (referred to as an agent) as a circle with radius R_i. We express agent i's position as the vector $\boldsymbol{r_i}$ and her velocity as the vector $\boldsymbol{v_i}$. There are two types of forces: a driving force $\boldsymbol{F_i}$, which propels the i^{th} agent (further referred to as *our agent*) toward her destination, and an interaction force $\boldsymbol{F_{ij}}$, which repels our agent from the j^{th} agent or environmental obstacle in an effort to maintain "personal space" (some SFM variations adapt this force to also represent attractive forces, like

shop windows and food stands) [3]. To simplify the problem, we only discuss interactions between agents.

Conveniently, both models use the same formula for the driving force.

$$\boldsymbol{F_i} = \frac{1}{\tau_0}\left(v_i^0 \boldsymbol{e_i^0} - \boldsymbol{v_i}\right) m_i$$

It can be thought of as the force required to accelerate the mass m_i from the current velocity $\boldsymbol{v_i}$ to the desired speed v_i^0 in the desired direction $\boldsymbol{e_i^0}$ over a *relaxation time* interval τ_0. This approach has seen extensive use in crowd models over the years, enough to reach a general consensus of $\tau_0 \approx 0.5s$ [3,6,9,13], however we found in our context $\tau_0 = 0.635s$. Note that $\boldsymbol{e_i^0}$ is a function of only the current position and velocity, that is, an agent's goal is static throughout time.

3.1 The Social Force Model

There are many versions of the Social Force Model (SFM), but we focused on the two most prominent: the circular (CSFM) and the elliptical (ESFM). The equations that followed are taken from [3].

3.1.1 The Circular SFM The original of the two versions, the CSFM uses an interaction force that is a function of the distance vector pointing from agent *j* to agent *i*, $\boldsymbol{d_{ij}} = \boldsymbol{r_i} - \boldsymbol{r_j}$, and is expressed as

$$\boldsymbol{F_{ij}} = A_i e^{-\boldsymbol{d_{ij}}/B_i} \frac{\boldsymbol{d_{ij}}}{\left\|\boldsymbol{d_{ij}}\right\|}$$

where A_i is a parameter reflecting the *interaction strength* and B_i is a parameter reflecting the *interaction range*. In simulation practice, a homogenous population is assumed by setting $A_i = A$ and $B_i = B$.

A major disadvantage of the CSFM is that the interaction force only depends on the distance between agents, $\boldsymbol{F_{ij}} = f\left(\boldsymbol{d_{ij}}\right)$. This may not always reflect reality as observed data has suggested that velocity is a factor in pedestrian behavior [3]. Also, agents tend to bounce off of each other as opposed to *sliding past*, which is the problem the ESFM aims to solve.

3.1.2 The Elliptical SFM This model was proposed to include a velocity dependence, as well as a force that is not strictly directed from agent *j* to agent *i* but instead includes a lateral component. Agents tend not to repel each other in the normal direction, but to *slide* past each other. There have been two noteworthy specifications of the Elliptical SFM [9].

In both specifications, the interaction potential is assumed to follow an exponentially decreasing function of the form $V(b_{ij}) = ABe^{-b_{ij}/B}$.

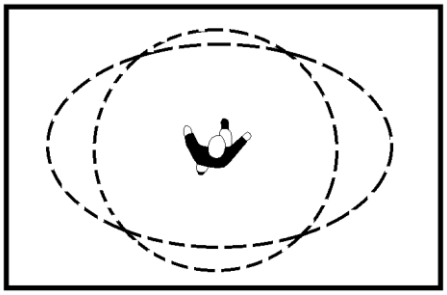

Figure 1: Illustration of the *regions of influence* of the circular and elliptical SFMs.

3.1.2.1 Elliptical Specification I considers the separation distance, as well as the velocity of the opposing agent. Here, the variable

$$b_{ij} = \frac{1}{2}\sqrt{(\|\boldsymbol{d_{ij}}\| + \|\boldsymbol{d_{ij}} - (\boldsymbol{v_j})\Delta t\|)^2 - \|(\boldsymbol{v_j})\Delta t\|^2}$$

represents the semi-minor axis of the elliptical equipotential lines (visualized as a *region of influence* illustrated in Figure 1). When expanded, the following explicit formula results.

$$\boldsymbol{F_{ij}} = -\nabla_{d_{ij}} ABe^{-b_{ij}/B} = Ae^{-b_{ij}/B} * \frac{\|\boldsymbol{d_{ij}}\| + \|\boldsymbol{d_{ij}} - \boldsymbol{y_{ij}}\|}{4\boldsymbol{b_{ij}}} * \left(\frac{\boldsymbol{d_{ij}}}{\|\boldsymbol{d_{ij}}\|} - \frac{\boldsymbol{d_{ij}} - \boldsymbol{y_{ij}}}{\|\boldsymbol{d_{ij}} - \boldsymbol{y_{ij}}\|}\right)$$

$$\text{where } \boldsymbol{y_{ij}} = \boldsymbol{v_j}\Delta t$$

3.1.2.2 Elliptical Specification II also considers the velocity of the focal agent and exhibits better accuracy than the aforementioned elliptical specification.

$$b_{ij} = \frac{1}{2}\sqrt{(\|\boldsymbol{d_{ij}}\| + \|\boldsymbol{d_{ij}} - (\boldsymbol{v_j} - \boldsymbol{v_i})\Delta t\|)^2 - \|(\boldsymbol{v_j} - \boldsymbol{v_i})\Delta t\|^2}$$

$$\boldsymbol{F_{ij}} = -\nabla_{d_{ij}} ABe^{-b_{ij}/B} = Ae^{-b_{ij}/B} * \frac{\|\boldsymbol{d_{ij}}\| + \|\boldsymbol{d_{ij}} - \boldsymbol{y_{ij}}\|}{4\boldsymbol{b_{ij}}} * \left(\frac{\boldsymbol{d_{ij}}}{\|\boldsymbol{d_{ij}}\|} - \frac{\boldsymbol{d_{ij}} - \boldsymbol{y_{ij}}}{\|\boldsymbol{d_{ij}} - \boldsymbol{y_{ij}}\|}\right)$$

$$\text{where } \boldsymbol{y_{ij}} = (\boldsymbol{v_j} - \boldsymbol{v_i})\Delta t$$

3.1.3 Anisotropy As they are, interaction forces in the two models are isotropic and result in agents reacting to forces equally from all directions. An anisotropic prefactor w_{ij} was proposed and partially incorporates the role of perception, in the form of vision, into the interaction forces as agents are typically less responsive to forces coming from behind. It is a function of the parameter $0 < \lambda_i < 1$ and the angle of incidence φ_{ij}.

$$w_{ij} = \lambda_i + (1 - \lambda_i)\frac{1+\cos(\varphi_{ij})}{2} \qquad \text{where } \cos(\varphi_{ij}) = \frac{v_i}{\|v_i\|} * \frac{-d_{ij}}{\|d_{ij}\|}$$

Although this effect is minimal in our head-on situation, anisotropy was considered as it is presented as a separate model in [9].

3.2 Physical Interactions

The above models are appropriate with a relatively sparse population. However, as crowd density increases the physical interactions between agents become significant. This is the subject of [10], and was consulted during this project.

3.3 The Universal Power Law

As opposed to the interaction force being a function of agent separation and velocity, the Universal Power Law (UPL) considers the *time to collision* τ. This anticipatory variable incorporates human cognition into the model, and is used to calculate a Boltzmann-like interaction force. The equations that follow are taken from [6,7]. UPL uses the same driving force F_i as the Social Force Model.

$$\tau = \frac{b-\sqrt{d}}{a}$$

where

$$a = \|\boldsymbol{v_{ij}}\|^2 \qquad b = -\boldsymbol{x_{ij}} \cdot \boldsymbol{v_{ij}} \qquad c = \|\boldsymbol{x_{ij}}\|^2 - (R_i + R_j)^2 \qquad d = b^2 - ac$$

$$\boldsymbol{x_{ij}} = \boldsymbol{x_i} - \boldsymbol{x_j} \qquad \boldsymbol{v_{ij}} = \boldsymbol{v_i} - \boldsymbol{v_j}$$

3.3.1 The UPL Interaction Force This model originates from the assumption that (agent) entropy is maximized throughout the system due to the observation that the system remains at constant statistical equilibrium (in terms of density and agent speed). An interaction potential $V(\tau) = \frac{k}{\tau^m} e^{-\tau/\tau_0}$, where *m* is a scalar parameter of the power law and *k* is a parameter that sets the units for energy. The authors used $m = 2 \; and \; k = 1.5$ [6,7], although the appropriateness of these parameters was not validated. The UPL interaction force is shown below.

$$\boldsymbol{F_{ij}} = -\nabla_{d_{ij}} \frac{k}{\tau^m} e^{-\frac{\tau}{\tau_0}}$$

$$= -\left[\frac{k e^{-\frac{\tau}{\tau_0}}}{\|\boldsymbol{v_{ij}}\|^2 \tau^2}\left(\frac{2}{\tau} + \frac{1}{\tau_0}\right)\right]\left[\boldsymbol{v_{ij}} - \frac{\|\boldsymbol{v_{ij}}\|^2 \boldsymbol{x_{ij}} - (\boldsymbol{x_{ij}} * \boldsymbol{v_{ij}})}{\sqrt{(\boldsymbol{x_{ij}} * \boldsymbol{v_{ij}}) - \|\boldsymbol{v_{ij}}\|^2 \left(\|\boldsymbol{x_{ij}}\|^2 - (R_i + R_j)^2\right)}}\right]$$

3.4 Discussion of Modified Social Force Model

Although it significantly differs from the SFMs and was therefore not included in my analysis, it is necessary to discuss a newly proposed amalgamation of the two models discussed [11]. In this model, the *time headway* H_{ij} is defined as the time for an agent i to collide with the current position of another agent j, that is the time to collision if the other agent were frozen in their current position. It has been observed that *time headway* remains approximately constant in normal situations. If the smallest time headway between the focal agent and all other agents and obstacles is less than some parameter H^T, then the agent reduces her speed to avoid the collision.

$$\boldsymbol{F_{Si}^H} = -m_i \frac{\boldsymbol{v_i^0}}{\tau_0}$$

When this force is active (i.e. when minimum *time headway* < H^T), its combination with the driving force $\boldsymbol{F_i}$ yields a force equal to $-m_i \frac{v_i}{\tau}$. This combination represents the desire to slow down to avoid collisions, as opposed to steering around them. Note that it negates the driving force, which can be thought of as introducing a variable desired destination.

Similar to UPL, our agent will experience an additional force $\boldsymbol{F_{Sij}^C}$ in the event that the *time to collision* (TTC) is nonzero and smaller than some threshold C^T. This force represents agent's i desire to resist increases in relative speed in the normal direction, that is it may alter the agent's speed as well as direction of travel.

$$\boldsymbol{F_{Sij}^C} = -m_i \frac{\boldsymbol{v_{ij} \cdot n_{i'j'}}}{\tau} \boldsymbol{n_{i'j'}} \quad \text{where } i' \text{ and } j' \text{ indicate future positions of the agents}$$

Calculations of the *time to collision* and *time headway* are presented in Appendix A.

4.0 PARAMETER CALIBRATION

The performance of crowd models largely depends on the suitable choice of parameters. Even with a finely calibrated model, the effects of new conditions on model parameters cannot be known *a priori*. However, previous model calibrations and insights from new data be used to make inferences about these effects. Several methods to quantify model fitness have been developed [3,7,9]. The latter serves as inspiration for this analysis. Johansson, Helbing, & Shukla (2008) produced optimized ranges of parameter values and their corresponding average "fitness" to a set of video recordings data (of low, medium, and high agent density) [9]. These ranges serve as a benchmark for my analysis and are shown in Table 1.

Model	A	B	λ	Fitness
Extrapolation	0	-	-	-0.66
Circular	0.42 ± 0.26	1.651 ± 1.01	0.12 ± 0.07	-0.6
Elliptical I	0.11 ± 0.01	1.19 ± 0.45	0.16 ± 0.04	-0.59
Elliptical II	0.04 ± 0.01	3.22 ± 0.67	0.06 ± 0.04	-0.39
Circular	0.11 ± 0.06	0.84 ± 0.63	1	-0.65
Elliptical I	1.52 ± 1.65	0.21 ± 0.08	1	-0.67
Elliptical II	4.30 ± 3.91	1.07 ± 1.35	1	-0.47

Table 1: Optimal parameter ranges as defined in Johansson et al., 2008.

4.1 Calibration Approach

The calibration approach was designed to represent the cases with the above parameter values. However, an important variable which is usually held constant in any particular model is the time-step Δt. To remove potential discrepancies when comparing the models, a curve was fit to the observed data to allow for the use of any Δt in the simulations. Several modifications to deal with computational problems were implemented, while remaining true to the method used in [9].

4.2.1 Effects of the Time-Step Value According to an email exchange with Stephen J. Guy, one of the authors of UPL (2014), the effects of the value chosen for Δt is much more prominent with UPL than the SFMs. In his experience UPL gives good results with $0.001s < \Delta t_{UPL} < 0.005s$, while SFM is simulated with $0.05s < \Delta t_{SFM} < 0.25s$. This agrees with trends I have read in other papers [3,6,9,10,11]. The time-steps of the videos we observed datasets were $\Delta t_{EMP} \approx 0.03667$s (~27 fps), which would raise concern about the role of Δt as a model parameter if used in the simulations. A curve was fitted using B-spline to the experimental data to get values at the appropriate time intervals.

4.2.2 B-Spline Curve Fitting To compare simulated data points with t values not present in the observed data set, B-spline curves corresponding to the observed $x_n(t)$ and $y_n(t)\ \forall\ n \in \{1,2,\dots,43\}$ were fit using SPLINEFIT in MATLAB. Data points were generated to match the timesteps in the simulations from these curves.

B-spline curve accuracy depends on the degree and number of breaks. We chose a linear fit with 1 break for $x_n(t)$ and a quadratic fit with 6 breaks for $y_n(t)$. Appendix B shows several plots of data and B-spline curves with varying degrees and number of breaks.

4.3 Model Fitness

The model fitness is defined as the average ratio of expected to simulated displacement for a single agent over all $N = 43$ simulation runs.

One minus the average ratio of the displacement error to the expected (splined) displacement was then averaged again over all ($N = 43$) simulation runs. This forms the fitness of a single (A, B, λ) parameter set.

$$U_{A_iB_i\lambda_i} = \frac{1}{43}\sum_{n=1}^{43}\left(1 - \frac{1}{K}\sum_{k=1}^{K}\frac{\left\|r_n^{simulated}(t_k+\Delta t) - r_n^{spline}(t_k+\Delta t)\right\|}{\left\|r_n^{spline}(t_k+\Delta t) - r_n^{spline}(t_k)\right\|}\right)$$

$$\text{where } \{t_k \in (t_0, T):\ r_n^{spline}(t_k+\Delta t) > r_n^{spline}(t_k)\}$$

4.4 Computational Considerations and Sources of Error

The boundaries of the B-spline curves are often less accurate than the interior, so a uniformly distributed random sample ($n = 80$) of data points were collected from the inner 75% of each timespan. To capture an accurate representation, this sample should be evenly spaced. However, the displacement changes were often so small that our video data was unable to capture these changes and sometimes resulted in a denominator of zero. The fitness calculation was repeated 50 times and the average taken as the "true" fitness.

5.0 SIMULATION RESULTS and FINDINGS

The two models were simulated in Visual C++ and their fitness was analyzed in MATLAB. I chose a $\Delta t_{SFM} = 0.1s$ for all SFM models and $\Delta t_{UPL} = 0.005s$ for UPL, which is consistent with most literature. Our empirical data suggests the desired velocity $v_i^0 = 1.5m/s$, which is slightly higher than in common literature.

One of the important characteristics of the SFM is that interaction forces are mostly normal. Although the ESFM models aim to correct this, in our head-on situation all SFMs failed to accurately replicate our empirical data. The agents engaged in a stalemate for several seconds until finally passing each other.

The parameter A represents the *interaction strength*, which when $A = 0$ causes an absence of interaction forces and yielded the highest fitness at $U_{CSFM,ESFMs} \approx -4.20$. When A is moderately increased to 0.1, the resulting fitness decreases to $U_{CSFM,ESFMs} = -32.0$. The fitness of anisotropic (when $\lambda \neq 0$) and isotropic SFM's showed no significant difference.

6.0 RECOMMENDATIONS for FUTURE WORK

As the SFMs are based on pedestrians' desire to maintain personal space, it is intuitive to theorize that its parameters would differ among cultures. This can be evidenced by the discussion of culture and the innate mind [14]. However, the detectability of these differences is situation-dependent. We cannot make any claims about the SFMs' robustness to cultural factors based at the moment, and more complex scenarios will be required to compare it to UPL.

The modified SFM uses a variable driving force, which could prevent the agents from engaging in a stalemate. It also resembles UPL in that it considers the time to collision. It is much less documented in current literature, but may be worth pursuing further.

7.0 ACKNOWLEDGMENTS

This work was accomplished during summer 2017 while I was working as a research internship at IIT Kanpur, India. I'd like to thank Dr. Shankar Prawesh and Dr. Indranil S. Dalal for their guidance and support.

8.0 APPENDIX A

$$H_{ij} = \max\left\{0, \frac{\|\boldsymbol{d_{ij}}\|\cos\theta_{ij} - \sqrt{(R_i+R_j)^2 - (\|\boldsymbol{d_{ij}}\|\sin\theta_{ij})^2}}{\|\boldsymbol{v_i}\|}\right\} \quad \text{where } \theta_{ij} = \cos^{-1}\left(\frac{\boldsymbol{v_i}}{\|\boldsymbol{v_i}\|}\cdot\frac{-\boldsymbol{d_{ij}}}{\|\boldsymbol{d_{ij}}\|}\right)$$

$$C_{ij} = \max\left\{0, \frac{\|\boldsymbol{d_{ij}}\|\cos\psi_{ij} - \sqrt{(R_i+R_j)^2 - (\|\boldsymbol{d_{ij}}\|\sin\psi_{ij})^2}}{\|\boldsymbol{v_{ij}}\|}\right\} \quad \text{where } \psi_{ij} = \cos^{-1}\left(\frac{\boldsymbol{v_{ij}}}{\|\boldsymbol{v_{ij}}\|}\cdot\frac{-\boldsymbol{d_{ij}}}{\|\boldsymbol{d_{ij}}\|}\right)$$

9.0 APPENDIX B

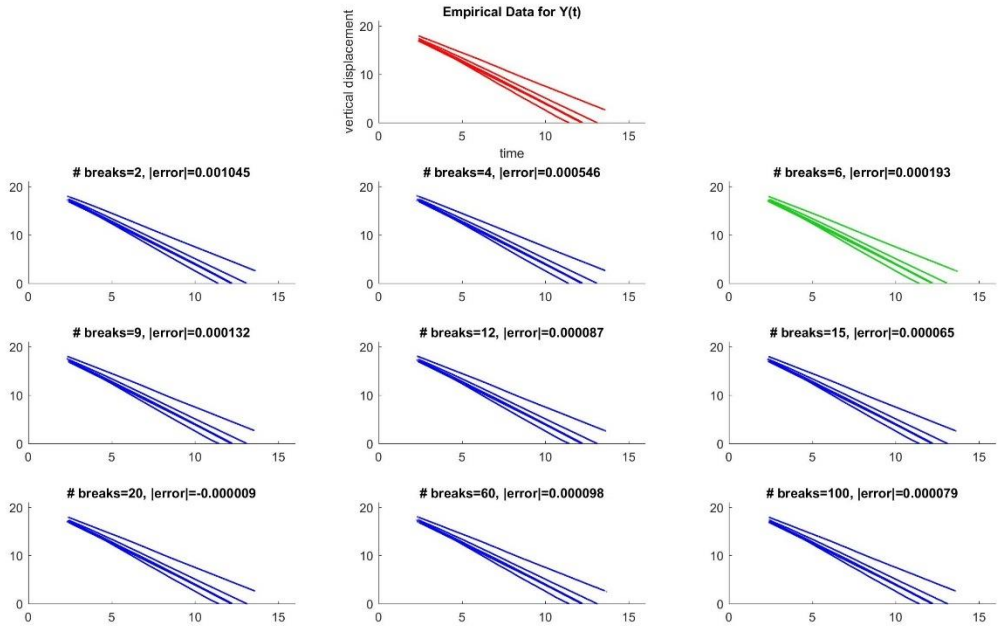

Figure 2: A sample of various B-splines for the horizontal displacement x(t).

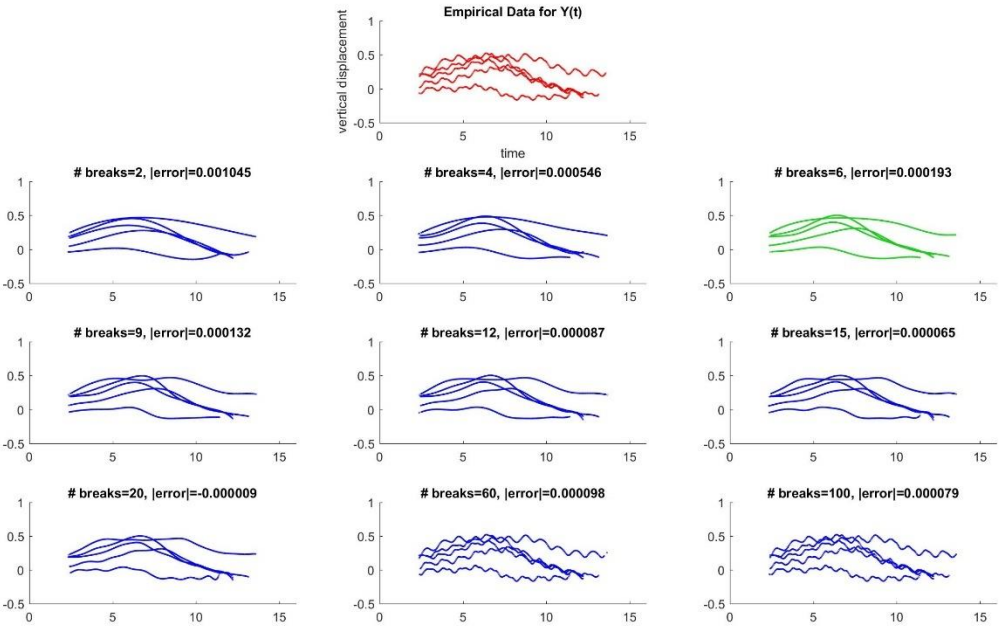

Figure 3: A sample of various B-splines for the vertical displacement y(t).

9.0 REFERENCES

[1] Helbing, Dirk, and Peter Molnar. "Social force model for pedestrian dynamics." Physical Review E (1995): 4282-4286. Web. 9 July 2017.

[2] Henderson LF (1974) On the fluid mechanics of human crowd motion. Transp Res 8:509–515

[3] Helbing, Dirk and Anders Johansson. “Pedestrian, Crowd, and Evacuation Dynamics.” Pedestrian, Crowd, and Evacuation Dynamics. 6476-6495. Web. 12 June 2017.

[4] Borgers A, Timmermans H (1986) City centre entry points, store location patterns and pedestrian route choice behaviour: A microlevel simulation model. Socio-Econ Plan Sci 20:25–31

[5] Gopal S, Smith TR (1990) NAVIGATOR: An AI-based model of human way-finding in an urban environment. In: Fischer MM, Nijkamp P, Papageorgiou YY (eds) Spatial choices and processes. North-Holland, Amsterdam, pp 169–200

[6] Karamouzas, Ioannis, and Brian Skinner and Stephen J. Guy. “A universal power law governing pedestrian interactions.” 9 Nov 2014. Web. 20 May 2017.

[7] Karamouzas, Ioannis, and Brian Skinner and Stephen J. Guy. “Supplemental material for: Universal Power Law Governing Pedestrian Interactions.” 9 Nov 2014. Web. 20 May 2017.

[8] Corbetta, Alessandro, and Adrian Muntean and Kiamars Vafayi. “Parameter Estimation of Social Forces in Pedestrian Dynamics via a Probabilistic Method.” Mathematical Biosciences and Engineering. Vol 12, Num 2, April 2015. Web. 4 July 2017.

[9] Johansson, Anders, and Dirk Helbing and Pradyumn K. Shukla. “Specification of a Microscopic Pedestrian Model by Evolutionary Adjustment to Video Tracking Data.” Advances in Complex Systems. World Scientific Publishing Company. 25 Oct 2008. Web. 8 July 2017.

[10] Helbing, Dirk, and Illes Farkas, and Tamas Vicsek. “Simulating dynamical features of escape panic.” Nature. 21 July 2000. Web. 25 May 2017.

[11] Gao, Yuan, and Tao Chen, and Hui Zhang, and Peter B. Luh. “Modified Social Force Model Based on Predictive Collision Avoidance Considering Degree of Competitiveness.” Fire Technology, 53, 331-351, 2017. Web. 8 July 2017.

[12] Hero5 Black. *GoPro.* N.p. N.d. Web. 12 July 2017.

[13] Curtis, Sean, and Andrew Best, and Dinesh Manocha. “Menge: A Modular Framework for Simulating Crowd Movement.” Collective Dynamics. N.d. Web. 1 June 2017.

[14] Simpson, Tom, Stephen Stitch, Peter Carruthers, and Stephen Laurence. Introduction to Culture and the Innate Mind. N.p., n.d. Web. 16 July 2017.